Toward Understanding the Catalytic Synergy in the Design of Bimetallic Molecular Sieves for Selective Aerobic Oxidations

Rebecca M. Leithall,[†] Vasudev N. Shetti,[§,‡] Sara Maurelli,[§] Mario Chiesa,[§] Enrica Gianotti,[⊥,§] and Robert Raja*,[†]

[†]School of Chemistry, University of Southampton, Southampton SO17 1BJ, U.K.
[§]Department of Chemistry and NIS-Centre of Excellence, University of Turin, 10125 Turin, Italy
[⊥]Dipartimento di Scienze e Innovazione Tecnologica, Centro Interdisciplinare Nano-SiSTeMI, Università del Piemonte Orientale, 15100 Alessandria, Italy

S *Supporting Information*

ABSTRACT: Structure−property correlations and mechanistic implications are important in the design of single-site catalysts for the activation of molecular oxygen. In this study we rationalize trends in catalytic synergy to elucidate the nature of the active site through structural and spectroscopic correlations. In particular, the redox behavior and coordination geometry in isomorphously substituted, bimetallic VTiAlPO-5 catalysts are investigated with a view to specifically engineering and enhancing their reactivity and selectivity in aerobic oxidations. By using a combination of HYSCORE EPR and *in situ* FTIR studies, we show that the well-defined and isolated oxophilic tetrahedral titanium centers coupled with redox-active VO^{2+} ions at proximal framework positions provide the loci for the activation of oxidant that leads to a concomitant increase in catalytic activity compared to analogous monometallic systems.

Figure 1. Schematic representation of the AlPO-5 framework where V and Ti ions have been incorporated as isomorphous replacements for Al^{3+} and P^{5+} ions, in alternating PO_4 and AlO_4 tetrahedra.

It is widely recognized that tetrahedrally coordinated Ti(IV) centers in titanium silicate-1 (TS-1) and Ti-MCM-41 possess well-defined, single sites for activating a range of hydrocarbons and aromatics using hydrogen peroxide (H_2O_2) and alkyl hydroperoxides (e.g., *tert*-butyl hydroperoxide) as oxidants.[1−3] Analogous titanium sites can also be incorporated through isomorphous substitution of T-site atoms with Ti(IV) ions in the strictly alternating PO_4 and AlO_4 tetrahedra of aluminophosphate (AlPO) molecular sieves.[4] The activity of these catalytic centers can be further enhanced by engineering a second, redox-active site via simultaneous incorporation of two different transition-metal ions (e.g., $Co^{III}Ti^{IV}AlPO-5$).[5] While these latter monometallic and bimetallic Ti-containing catalysts have proved effective in the oxidation of olefins using H_2O_2[6] and acetylperoxyborate (APB) as oxidants,[7,8] there are very few reports outlining their efficacy for activating molecular oxygen in selective oxidation reactions.

Engineering two cooperative components into a catalyst is often interpreted as either support−metal synergy (for effective anchoring)[9] or metal−metal synergy (e.g., bifunctionality).[10] For example, it was shown[11] that ruthenium and tin active sites supported (by impregnation and deposition methods) on 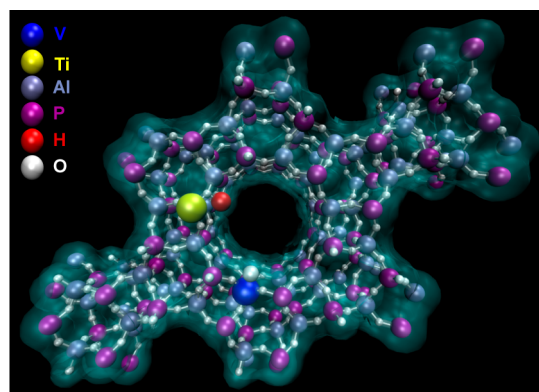γ-alumina exhibit synergistic enhancements in both catalytic activity and selectivity: the oxophilic tetrahedral Sn sites alter the polarization of the carbonyl bonds (via Sn−O interactions), thereby facilitating Ru−H hydride transfers in the hydrogenation of cinnamaldehyde. While there is an abundance of literature for enabling such synergistic interactions using metal nanoparticles[12] and post-synthesis modification/impregnation techniques,[13] there are relatively very few examples[7] for generating multimetallic, isolated active sites through simultaneous isomorphous framework substitution. Understanding the specific loci and interactions of metal centers allows structure−property correlations to be established, which can be utilized in a strategic design−application approach to catalysis. Metal environments and coordination geometry can be probed by a number of sophisticated spectroscopic techniques, such as MAS NMR,[14,15] EPR, and UV/vis,[16] which have enabled the specific localization of active metal centers to be mapped and the intrinsic role of the active site to be deduced.

In this investigation we have specifically devised a synthetic strategy where the local structural environment, redox behavior, and coordination geometry of the bimetallic species (V−Ti) can be precisely controlled, so that the nature of the active site and its implicit role in the catalytic process can be ascertained

through spectroscopic characterization (diffuse reflectance (DR) UV/vis, FTIR, and EPR), thereby enabling structure–property correlations to be established. This has, in turn, facilitated the evaluation of its catalytic potential in reactions involving molecular oxygen as the oxidant, which have paved the way for exploring the potential of these materials in industrially significant catalytic transformations from the standpoint of sustainable catalysis.

Bimetallic VTiAlPO-5 catalysts were synthesized (see Supporting Information section SI1 for full synthesis details) by adapting and suitably modifying previously reported procedures,[5] using a gel ratio of 0.97 Al:1.5 P:0.03 M: 0.03 Ti:0.8 SDA:50 H_2O, where M is the complementary redox metal and the structure-directing agent (SDA) is *N*-methyldicyclohexylamine.[17] For comparison, monometallic (V, Ti) and analogous bimetallic equivalents of $Co^{III}Ti^{IV}AlPO$-5 and $Mn^{III}Ti^{IV}AlPO$-5 were synthesized, and their phase purity was confirmed using powder X-ray diffraction, which resulted in diffractograms characteristic of the AFI framework,[18] with a high degree of crystallinity and no mixed-phase impurities (see Figure SI2.1 for patterns and Table SI2.2 for associated Reitveld refinements). Inductively coupled plasma resonance was used to compare the theoretical loadings of the metals in the synthesis gel and the final calcined samples (Tables SI1.1 and 3.1). All of the metals used in this study gave a good agreement between the intended loading and the final composition, with the exception of vanadium, where ~69% of the metal was incorporated into the final structure. We believe that the vanadyl molecular ion (V=O), as observed by EPR spectroscopy (see later), has a square-pyramidal geometry, which might somewhat limit the isomorphous replacement of the tetrahedral Al site, thereby restricting the extent of incorporation of the vanadium species in the AFI framework.

Brunauer–Emmett–Teller measurements (see Table SI3.1) gave consistent internal pore surface areas and were in good agreement with literature values.[6] Sample morphology was assessed using scanning electron microscopy (Figure SI3.1), showing uniform spherical particles with an average size of 10–20 μm (see SI3 for physico-chemical characterization data). The catalytic potential of the three bimetallic catalysts was initially evaluated in the epoxidation of cyclohexene, using reaction conditions analogous to those reported earlier[5] for the $Co^{III}Ti^{IV}AlPO$-5 system, with a view to establishing a comparative reactivity profile. It was indeed surprising that the VTiAlPO-5 catalyst exhibits superior catalytic performance (over twice the conversion of cyclohexene to its epoxide: 30.5% for CoTiAlPO-5 versus 63.4% for VTiAlPO-5 after 3 h; see Table SI4.1 for full details) compared with its analogous counterparts (Figure 2A). APB was used as the oxidant of choice in these reactions, as redox centers (such as Mn(III) and Co(III)) are believed[19,20] to promote the formation of the active oxygen species to the reaction sphere. Moreover, combining this effective oxidant and the size selectivity of the AlPO-5 channels facilitates high selectivities (in excess of 98%) toward the target cyclohexene epoxide, thereby affording the prospect to probe the origins of the enhanced turnovers in greater depth. (See Figure SI4.3B for oxidant selectivity profiles.)

To further substantiate the efficacy of the bimetallic substitution, we evaluated the performances of the individual (V and Ti) monometallic analogues, which were inferior to the bimetallic catalyst (Figure 2B). Interestingly, the performance of the physical mixture (containing identical moles of the
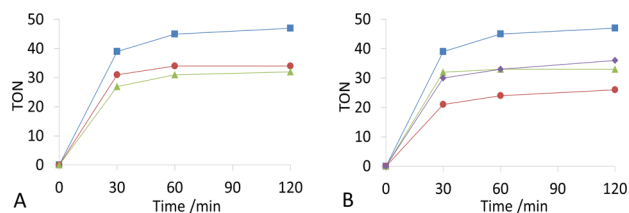

Figure 2. (A) Comparison of turnover numbers (TON) for the epoxidation of cyclohexene using bimetallic catalysts: blue squares, VTiAlPO-5; red circles, CoTiAlPO-5; green triangles, MnTiAlPO-5. (B) Relative performance (TON) of monometallic and bimetallic V–Ti catalysts in the epoxidation of cyclohexene: blue squares, VTiAlPO-5; red circles, monometallic VAlPO-5; green triangles, monometallic TiAlPO-5; purple diamonds, physical mixture of VAlPO-5 and TiAlPO-5. Catalysis was carried out at 338 K and atmospheric pressure using dichloromethane as the solvent; oxidant:substrate ratio = 1.1:1. See SI4 for full experimental conditions.

individual metals to mirror the composition of the bimetallic VTiAlPO-5 catalyst) of the two monometallic analogues is significantly worse than its bimetallic counterpart. This strongly suggests that the two active centers, when isomorphously incorporated into the same framework, exhibit a cooperative or synergistic influence, which facilitates an effective interaction between the substrate and oxidant that minimizes wasteful decomposition of the latter. The heterogeneous nature of all the catalysts was scrutinized by running recycle tests (see Figure SI4.3A) and stringently analyzing the reaction mixture using atomic absorption spectroscopy, which revealed only trace quantities (<3 ppb) of metal, thereby eliminating any prospects of leaching of the active sites, which further augments the stability and recyclability of our catalysts.

To elucidate the nature and role of each of the metal sites in the AlPO-5 catalysts, detailed spectroscopic characterization by DR UV/vis (see Figure SI5.1) and FTIR spectroscopies, using CO as a probe molecule, was carried out (see Figure SI6.1). To study the redox properties of the metals (Co, V, and Mn), the catalysts were reduced in H_2 at 673 K and subsequently oxidized in O_2 at 823 K.

In the UV range (270–290 nm), the VTiAlPO-5 oxidized catalyst (Figure 3A) displays an intense, broad band due to LMCT transitions of isolated T_d V(V) sites, providing direct evidence for incorporation of V into the AlPO-5 framework. The strong tail in the 350–450 nm range suggests the presence of some polymeric vanadium species, such as V_2O_5. After reduction, the band becomes sharper, with a maximum at 220–260 nm, assigned to LMCT transition of monomeric V(IV) in four- and five-fold coordination and to Ti(IV) centers. In addition, the weak bands at 530 and 660–1100 nm can be assigned to d-d transitions of T_d monomeric V(IV) centers.[21] In the FTIR spectra (Figure 3B), the band at 2195 cm^{-1}, which is only detected in the reduced sample, is due to CO adsorbed on vanadyl species,[22] further substantiating that the vast majority of V(IV) sites are converted into V(V) centers upon oxidation. The titanium sites in the bimetallic AlPO-5 catalysts were detected by complete reduction of the catalysts in H_2 at 673 K to eliminate the overlap of the intense UV bands of V(V) with those of Ti(IV) (Figure 3A inset). VTiAlPO-5 displays a strong shoulder at 215 nm, attributed to isolated tetrahedral Ti(IV) LMCT transitions. The maximum at 245 nm is likely to have some contributions from both Ti(IV) and V(V) isolated sites.[23]
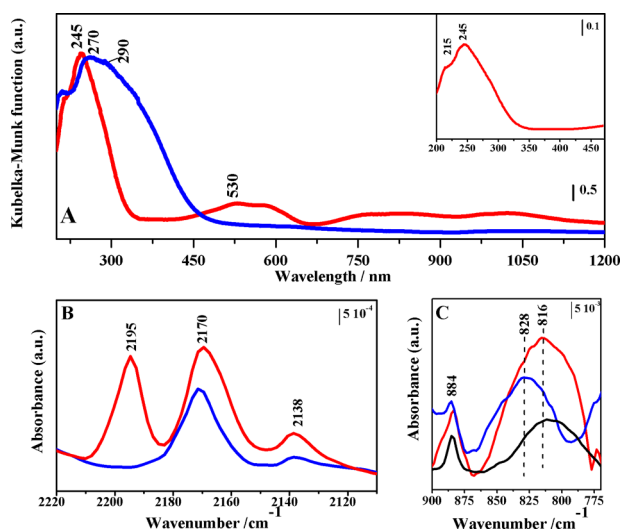
Figure 3. (A) DR UV/vis spectra of oxidized (blue) and reduced (red) VTiAlPO-5; the inset shows the expanded spectrum of reduced VTiAlPO-5. (B) FTIR spectra of the oxidized (blue) and reduced (red) VTiAlPO-5, recorded at 80 K after CO adsorption (1 mbar). (C) FTIR spectra of oxidized VTiAlPO-5 (red), VAlPO-5 (blue), and TiAlPO-5 (black) recorded at 80 K after interaction with APB.
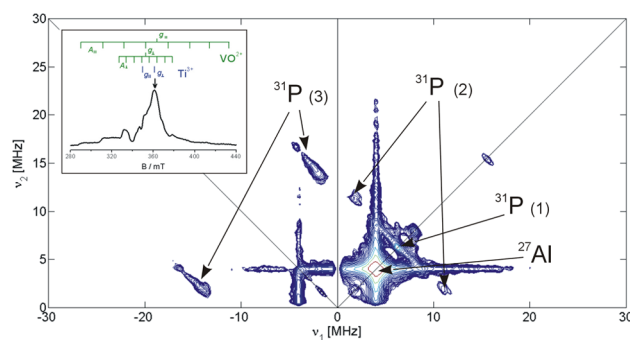
Figure 4. Experimental HYSCORE spectrum of reduced VTiAlPO-5 sample recorded at 10 K and observer position $B_0 = 362.0$ mT (arrow in the inset). The experimental ESE-detected EPR spectrum is shown in the inset. Stick diagrams indicate the contributions of VO^{2+} and Ti^{3+} species to the overall signal.

The interaction of the oxidant APB with the metal sites in the oxidized form was probed by *in situ* FTIR spectroscopy [ν(O−O) stretching mode] to better understand the nature of peroxo species formed during the catalytic reaction.[24] Upon interaction with APB (Figure 3C), under conditions identical to those used in the catalytic runs (reported in Figure 2), VTiAlPO-5 displays a weak band at 884 cm^{-1} and a broad, more intense signal at 816 cm^{-1}. The band at 884 cm^{-1}, also present in the spectra of TiAlPO-5 and VAlPO-5, is due to physisorbed APB, while that at 816 cm^{-1} is assigned to the stretching mode of O−O peroxo species. This band is not present in the spectrum of the undoped AlPO-5 sample (see Figure SI7.2) but is present in the spectra of monometallic TiAlPO-5 (centered at 816 cm^{-1}) and VAlPO-5 (at 828 cm^{-1}); in VTiAlPO-5 this band is broader, and both components can be directly attributed to peroxo species formed on Ti(IV) and V(V) sites. Furthermore, the presence of isolated, tetrahedral Ti(IV) sites and V(V) centers in VTiAlPO-5 catalyst synergistically enhances the formation of the peroxo species, which has a beneficial effect on its overall catalytic performance (shown in Figure 2).

To further clarify the local environment of the Ti and V ions in the AlPO-5 framework, pulse EPR experiments were carried out on the reduced system, where both species are in their paramagnetic states (V^{4+} and Ti^{3+} $3d^1$). The electron spin echo (ESE)-detected EPR spectrum of the reduced VTiAlPO-5 catalyst (Figure 4 inset) is characterized by a complex powder pattern extending over ~160 mT and characteristic of VO^{2+} ions in square-pyramidal coordination. Superimposed on this signal is a prominent absorption band characterized by a pseudo-axial **g** matrix ($g_{\parallel} = 1.991$ and $g_{\perp} = 1.908$), which can be firmly assigned to Ti^{3+} species subjected to a tetrahedral crystal field,[25] in good agreement with the UV/vis experiments.

Hyperfine sublevel correlation (HYSCORE) experiments were then carried out to measure the superhyperfine interactions of the unpaired electron on the metal cations with magnetically active nuclei of the AlPO lattice [^{31}P ($I = 1/2$), ^{27}Al ($I = 5/2$)]. A typical HYSCORE spectrum recorded at

field positions corresponding to the maximum absorption of the Ti^{3+} species is shown in Figure 4. The spectrum is analogous to that observed for the monometallic system (see SI8), and a detailed analysis has been reported elsewhere.[26] The spectrum features relatively strong ^{31}P hyperfine couplings, as indicated in Figure 4. This fact together with the absence of similar couplings to ^{27}Al nuclei unequivocally proves that Ti^{3+} ions are isomorphously substituted in the AlPO-5 framework at Al^{3+} positions. Similar spectra (Figure SI8.3) have been recorded at a field position where only VO^{2+} species resonate, indicating that a similar situation holds for VO^{2+} ions.

From these spectroscopic observations, it can be concluded that both the vanadium and titanium centers, when isomorphously (simultaneously) incorporated into the AFI framework, play distinct roles and act in a concerted fashion to synergistically boost the overall catalytic performance (Figure 2). The tetrahedral nature of the oxophilic titanium center is more likely to bind to the oxidant and activate it (through the formation of peroxo species, Figure 3C), as it is able to expand its coordination sphere, unlike the already saturated octahedral species observed in MnTiAlPO-5 (see Figure SI5.1). It could be further rationalized that, since the complementary redox center plays a significant role in the catalytic turnover, the vanadium ions, with a lower redox barrier, will more efficiently catalyze the reaction once a proximal titanium center has activated the oxidant (Figure 3B). We therefore probed the efficacy of this catalyst in the activation of molecular oxygen for the oxidation of benzyl alcohol and in a series of other related selective oxidations that are of high relevance in the chemical and fine-chemical industries.

Selective oxidation of benzyl alcohol to benzaldehyde is of paramount importance in the synthesis of a range of pharmaceutical intermediates (e.g., mandelic acid), plastic additives, photographic chemicals, and certain aniline dyes. Conventional industrial methods for the synthesis of related products (e.g., vanillin and terephthalic acid) involve the use of stoichiometric amounts of chromate, permanganate, Br_2/acetic acid, or tetra-*N*-propylammonium perruthenate/*N*-methylmorpholine-*N*-oxide as stoichiometric oxygen donors[27] and activators (to maximize selectivity), which generate copious quantities of metal waste and have serious toxicity issues associated with them.[28] Developing environmentally benign, atom-efficient, sustainable, catalytic methods that ideally utilize molecular oxygen as the oxidant for these selective trans-
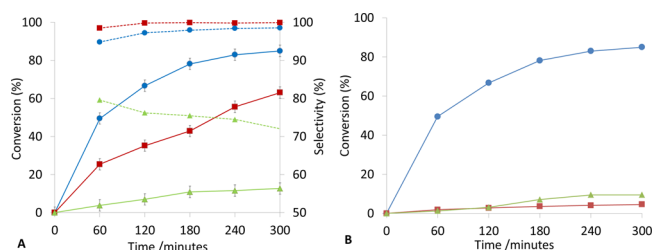
2917

dx.doi.org/10.1021/ja3119064 | *J. Am. Chem. Soc.* 2013, 135, 2915−2918

Figure 5. (A) Conversion (bold lines) and selectivity (dashed lines) for the aerobic oxidation of benzyl alcohol. Blue circles, VTiAlPO-5; red squares, VAlPO-5; green triangles, TiAlPO-5. (B) Comparison of the performance of bimetallic analogues in the aerobic oxidation of benzyl alcohol. Blue circles, VTiAlPO-5; red squares, CoTiAlPO-5; green triangles, MnTiAlPO-5. Catalysis carried out at 373 K at 2.0 MPa of air using *tert*-butanol as solvent. See SI4 for full experimental conditions.

formations is therefore of vital importance from economic and environmental viewpoints.

The catalytic results for the oxidation of benzyl alcohol, using molecular oxygen as the oxidant, with the monometallic and bimetallic VTi catalysts are summarized in Figure 5A. In line with earlier trends, the bimetallic catalyst far exceeds the performance of its corresponding monometallic analogues, further substantiating the concerted role of the redox-active vanadium and oxophilic (tetrahedral) titanium active centers for boosting the overall efficiency of the reaction. It is noteworthy that analogous bimetallic systems with a lower degree of redox efficiency[29,30] (e.g., CoTiAlPO-5) or less-pronounced tetrahedral character (e.g., MnTiAlPO-5) were inferior in performance to the corresponding VTi analogue (Figure 5B).

The full range of industrially significant oxidations that could be effected with these adroitly designed bimetallic catalysts and molecular oxygen is further highlighted in Figure SI4.7. While further optimization of process parameters and reaction conditions is currently underway, it is remarkable that vanillyl and cinnamyl alcohols were facilely oxidized using O_2 as the oxidant, under rather mild conditions, and displayed high catalytic turnovers (764 and 718 respectively), further substantiating the importance of the design strategy in effecting sustainable catalytic transformations both from academic and industrial perspectives.

ASSOCIATED CONTENT

Ⓢ Supporting Information

Additional characterization evidence and details of experimental methods. This material is available free of charge via the Internet at http://pubs.acs.org.

AUTHOR INFORMATION

Corresponding Author
rr3@soton.ac.uk

Present Address
‡Refinery R&D, Reliance Industries Ltd., Jamnagar, 361142, Gujarat, India

Notes
The authors declare no competing financial interest.

ACKNOWLEDGMENTS

REFERENCES

(1) Wang, Y.; Wang, G.; Yang, M.; Tan, L.; Dong, W.; Luck, R. *J. Colloid Interface Sci.* **2011**, *353*, 519.
(2) Guidotti, M.; Batonneau-Gener, I.; Gianotti, E.; Marchese, L.; Mignard, S.; Psaro, R.; Sgobba, M.; Ravasio, N. *Microporous Mesoporous Mater.* **2008**, *111*, 39.
(3) Zahedi-Niaki, M. H.; Kapoor, M. P.; Kaliaguine, S. *J. Catal.* **1998**, *177*, 231.
(4) Flanigen, E. M.; Lok, B. M.; Patton, L.; Wilson, S. T. *Pure Appl. Chem.* **1986**, *58*, 1351.
(5) Paterson, J.; Potter, M.; Gianotti, E.; Raja, R. *Chem. Commun.* **2011**, *47*, 517.
(6) Lee, S.-O.; Raja, R.; Harris, K. D. M.; Thomas, J. M.; Johnson, B. F. G.; Sankar, G. *Angew. Chem.* **2003**, *115*, 1558.
(7) Raja, R.; Thomas, J. M.; Xu, M.; Harris, K. D. M.; Greenhill-Hooper, M.; Quill, K. *Chem. Commun.* **2006**, 448.
(8) Raja, R.; Thomas, J. M.; Greenhill-Hooper, M.; Ley, S. V.; Paz, F. A. A. *Chem. Eur. J.* **2008**, *14*, 2340.
(9) Hermans, S.; Raja, R.; Thomas, J. M.; Johnson, B. F. G.; Sankar, G.; Gleeson, D. *Angew. Chem., Int. Ed.* **2001**, *40*, 1211.
(10) Thomas, J. M.; Raja, R. *Proc. Natl. Acad. Sci. U.S.A.* **2005**, *102*, 13732.
(11) Neri, G.; Mercadante, L.; Milone, C.; Pietropaolo, R.; Galvagno, S. *J. Mol. Catal. A: Chem.* **1996**, *108*, 41.
(12) Jiang, H.-L.; Xu, Q. *J. Mater. Chem.* **2011**, *21*, 13705.
(13) Choudhury, I. R.; Thybaut, J. W.; Balasubramanian, P.; Denayer, J. F. M.; Martens, J. A.; Marin, G. B. *Chem. Eng. Sci.* **2010**, *65*, 174.
(14) Mothe-Esteves, P.; Maciel Pereira, M.; Arichi, J.; Louis, B. *Cryst. Growth Des.* **2010**, *10*, 371.
(15) Olmos, A.; Rigolet, S.; Louis, B.; Pale, P. *J. Am. Chem. Soc.* **2012**, *116*, 13661.
(16) Smeets, P. J.; Woertink, J. S.; Sels, B. F.; Soloman, E. I.; Schoonheydt, R. A. *Inorg. Chem.* **2010**, *49*, 3573.
(17) Sánchez-Sánchez, M.; Sankar, G.; Simperler, A.; Bell, R. G.; Catlow, C. R. A.; Thomas, J. M. *Catal. Lett.* **2003**, *88*, 163.
(18) Figiel, P. J.; Sobczak, J. M. *J. Catal.* **2009**, *263*, 167.
(19) Roesler, R.; Schelle, S.; Gnann, M.; Zeiss, W. (Peroxid-Chemie GmbH). U.S. Patent 5462692, Oct 31, 1995.
(20) Raja, R.; Thomas, J. M.; Xu, M.; Harris, K., D, M.; Greenhill-Hooper, M.; Quill, K. *Chem. Commun.* **2006**, 448.
(21) Vishnuvarthan, M.; Gianotti, E.; Paterson, J.; Raja, R.; Piovano, A.; Bonino, F.; Berlier, G. *Microporous Mesoporous Mater.* **2011**, *138*, 167.
(22) Hadjiivanov, K. J.; Vayssilov, G. N. *Adv. Catal.* **2002**, *47*, 307.
(23) Lenoc, L.; On, D., T.; Solomykina, S.; Echchaed, B.; Beland, F.; Moulin, C. C. D.; Bonnevoit, L. *Stud. Surf. Sci. Catal.* **1996**, *101*, 611.
(24) Tozzola, G.; Mantegazza, M.; Ranghino, G.; Petrini, G.; Bordiga, S.; Ricchiardi, G.; Lamberti, C.; Zulian, R.; Zecchina, A. *J. Catal.* **1998**, *179*, 64.
(25) Maurelli, S.; Vishnuvarthan, M.; Chiesa, M.; Berlier, G.; Van Doorslaer, S. *J. Am. Chem. Soc.* **2011**, *133*, 7340.
(26) Maurelli, S.; Chiesa, M.; Giamello, E.; Leithall, R. M.; Raja, R. *Chem. Commun.* **2012**, *48*, 8700.
(27) Backvall, J. E. *Modern Oxidation Methods*; Wiley-VCH: Weinheim, 2005.
(28) Pillai, U. R.; Sahle-Demessie, E. *Appl. Catal., A* **2003**, *245*, 103.
(29) Berndt, H.; Martin, A.; Zhang, Y. *Microporous Mater.* **1996**, *6*, 1.
(30) Barrett, P. A.; Sankar, G.; Jones, R. H.; Catlow, C. R. A.; Thomas, J. M. *J. Phys. Chem. B* **1997**, *101*, 9555.